Risk-based Ship Hull Hybrid Structural Design and Optimisation Employing Genetic Algorithm

E. Koni
Instituto Superior Técnico, Universidade de Lisboa, Lisbon, Portugal

ABSTRACT: The optimum ship hull design solution has always been a concern, and in recent years genetic algorithms to optimise the ship hull structure have been developed. The genetic algorithm's fundaments generate alternative solutions and compare them with pre-defined constants and objectives. The development of design solutions evolves through competition and controlled variations. Minimising the ship hull structure weight is essential in reducing the ship's capital (construction) expenditure and increasing the cargo capacity. The risk of the ship is associated with the loss of the ship, cargo, human life, environmental pollution, etc. It is a governing factor impacted by the chosen structural design solution and the measures taken to reduce the structural weight. The master's degree thesis will employ a genetic algorithm to study the weight minimisation of a multi-purpose ship hull structure controlling the associated risk by accounting for several structural design variables. The probability of compressive collapse of the stiffened plates, integral ship hull structure and the associated cost due to failure is used as a base to define the risk and best design solution. The Pareto frontier solutions, calculated by the non-dominated sorting genetic algorithm, NSGA-II, will be employed to determine feasible solutions for the design variables. The first-order reliability method, FORM, will estimate the Beta reliability index based on the topology of the stiffened plates and ship hull structure as a part of the Pareto frontier solutions. The algorithm employed will not account for any manufacturing constraints and consequences due to the encountered optimal design solution.

1 INTRODUCTION

Ship design is a complex process due to the considerable number of technical aspects; their optimisation may be very different in the distinct stages of design and result in conflicting solutions.

With the development of recent technologies, many design tasks can be performed simultaneously, considering multiple technical aspects in the early design stages. This methodology, called Concurrent Engineering, has a positive impact on the optimisation of production, delivery time and, therefore, the costs along the ship's lifecycle, with an increased knowledge of the product at a preliminary stage.

The development of genetic algorithms (GAs) in recent years has contributed to the optimisation of the ship hull structure, with the possibility of integrating multiple criteria in the decision-making. Minimising the ship hull structural weight is essential in reducing the ship's capital (construction) expenditure and increasing the cargo capacity. The risk of the ship is associated with the loss of the ship, cargo, human life, environmental pollution, etc., a governing factor impacted by the chosen structural design solution and the measures taken to reduce the structural weight.

The advantage of GAs in ship hull structural optimisation is their ability to deal with highly non-linear problems. In this work, design variables, such as plate panel thicknesses, bulb profiles, span, aluminium honeycomb core density and materials, are discrete variables not dealt with in a standard linearisation approach involving gradients in the search process. Therefore, the complexity of this optimisation lies in translating the discrete nature of the design variables into a model, considering many constraints given by the Class Societies' Rules. With this respect, GAs allow obtaining a set of Pareto-optimum solutions which give a complete view of the problem, rather than applying classical approaches to obtain a single-point solution (Srinivas, et al., 1994). The obtained Pareto-optimal front allows the decision maker to compare multiple solutions as a function of additional measures of merit, in this case, the β-reliability index.

The International Maritime Organization (IMO) target to reduce greenhouse gas emissions from shipping by at least 50% in 2050 compared to 2008, plays a key role in the ship hull structural weight minimisation, considering that the maritime sector accounted for more than 3% of worldwide CO_2 emissions. The application of alternative design solutions, such as aluminium honeycomb structures (AHS), may reduce the hazardous and polluting emissions throughout the ship's lifecycle (Nepomuceno de Oliveira, et al., 2022). Aluminium is a versatile and recyclable material (Mahfoud & Emade, 2010). It can contribute to fuel savings, power reduction, increased cargo capacity and improvement of the Energy Efficiency Design Index (EEDI) for new ships (IMO, 2011).

However, potential applications of AHS to strength parts of the structure, such as the inner shell, are still limited due to the incapacity of AHS to resist axial compressive loads generated by the vertical bending moment.

The scope of this work is to contribute to the analysis of the potential advantages of AHS in hybrid ship hull structures, given future developments in understanding the interaction between steel plate panels and AHS panels.

2 STATE OF THE ART

2.1 *Ship structural design*

The development of innovative technologies over the past century has impacted the maritime industry, ranging from developments in shipbuilding and ships to ship structural design.

Before the development of finite element methods (FEM), ship hull structures were designed and dimensioned with empirical methods solely based on classification societies' rules, which were themselves the result of accumulated experience and feedback from ships in service. Based on this approach, the designer cannot quantify the influence of variables' change in a new design. Due to the missing functional link between input design variables and output design criteria, different variants cannot be analysed; therefore, the best design solution cannot be identified.

The development of finite element methods and computers introduced an increase in analysis capacities, making it possible to move to a rationally-based design approach (Hughes, et al., 1980). This design approach is directly and entirely based on the structural theory and computer-based methods of structural analysis and optimisation in achieving an optimum defined structure.

Rationally-based design is not automated; therefore, decisions (objectives, properties, criteria, constraints…) must be made before the design process. However, the two design approaches are complementary and employed were most appropriately. The latter is mainly used in a preliminary ship design phase where the principal dimensions are determined by a given set of requirements and limitations. On the other hand, empirical methods are particularly suitable for detail design and, due to a large number of local structural components, can be implemented in mass production (Hughes & Paik, 2010; Palaversa, et al., 2020).

2.2 *Limit states design*

Limit State Design (LSD) is a reliability-based design describing a state beyond which a structure no longer satisfies the requirements. For marine structures, this is subdivided into four categories: Serviceability limit state (SLS), Ultimate limit state (ULS), Fatigue limit state (FLS) and Accidental limit state (ALS) (IACS, 2021).

An accurate assessment of a structure's ultimate strength is not a trivial task due to the possible occurrence of high plastic strain regions, tripping phenomena, residual stresses, imperfections, etc. Research in this field follows three principal areas: empirical, analytical, and numerical methods (ISSC, 2003).

An essential contribution to the analytical derivation of the hull's ultimate strength came from Caldwell (1965). He considered the buckling in compression and yielding in tension, also considering the change of the neutral axis in the section. Paik and Mansour (1995) proposed an analytical formulation that also considered double-hull cross-sections and material properties of various steel plates by adapting the original Caldwell formulation.

Smith (1977) introduced a progressive collapse method to estimate the longitudinal strength of a ship's hull, on which Paik (2003) elaborated a particular purpose computer program (ALPS/HULL) for the progressive collapse analysis.

Recent studies on the ultimate strength assessment have been conducted by Tekgoz et al. (2015) on a containership, accounting for the effect of neutral axis movement, translation, and rotation. Further studies on strength assessment were presented by Tekgoz and Garbatov (2020; 2021).

2.3 *Reliability and risk-based design*

Reliability aspects started to be considered in aeronautics in the 1930s with the collection of statistical data on the failure of various components and aircraft engines (Rausand, 1998). These data were further studied to improve the design and possibly avoid accidents. By the end of the 1970s was applied to a wide range of industries, from oil to railway and car industries (Wang, 1994).

The measure of reliability by use of a reliability β-index was introduced by Cornell (1969). Hasofer and Lind (1974) proposed a First-order Reliability

Method (FORM) to calculate the β-index. Rackwitz (1978) and Fiessler proposed an algorithm to solve the constrained problem optimisation. Det Norske Veritas (DNV, 1992) contributed with a classification note on structural reliability analysis of marine structures.

Parunov and Guedes Soares (2008) considered the ultimate collapse bending moment of a converted Aframax oil tanker to quantify the change in notion reliability levels applying the FORM. Feng et al. (2015) performed a reliability assessment of three structural members of a bulk carrier on a direct strength calculation.

Risk assessment includes the study of the consequences of the failures of the item in terms of possible damage to property, injury/death of people, and/or the degradation of the environment (Wang, et al., 2004).

Two risk-assessment approaches are available: qualitative and quantitative risk assessment (Wang, 2006). Quantitative Risk Assessment (QRA) frameworks were first applied to Ro-Ro ferry safety in general by Spouge (1989). Wang et al. (1996) proposed an early application of QRA with a safety-based design and maintenance optimisation of large marine engineering systems. Garbatov et al. (2018) proposed a risk-based framework for ship and structural design accounting for maintenance planning.

2.4 *Lightweight structures*

Structural weight saving may become particularly important in specific types of lightweight transportation, and applying sandwich structures over the increase of material thickness may be preferable. These structures provide excellent structural efficiency in a high strength-to-weight ratio (Paik, et al., 1999), along with various benefits concerning mechanical properties, fire safety, manufacturing accuracy and fabrication price (Kujala & Klanac, 2005).

These structures have been initially adopted for small vessels and, for bigger ships, non-strength parts of structures due to various problems in applying dynamically loaded structures (Paik, et al., 1999). Practical applications on large vessels were realised from the 1990s onwards by the shipyard *Meyer Werft* on cruise ships (Kujala & Klanac, 2005).

Research on sandwich structures dates to the 1940s, dealing with the buckling of panels. The books of Plantema (1966) and Allen (1969) outlined the theory and analysis methodologies of sandwich structures, followed by the books of Zenkert (1993) and Vinson (1999). Experimental studies on buckling strength characteristics of aluminium honeycomb sandwich panels in axial compression were undertaken by Yeh and Wu (1991). Kobayashi et al. (1994) studied the elasto-plastic bending behaviour of sandwich panels. Paik et al. (1999) investigated the strength characteristics of aluminium honeycomb core sandwich panels based on the so-called equivalent plate thickness method (Okuto, et al., 1991).

The advantages of sandwich panels include potential applications for slamming impact alleviation (Qin & Batra, 2009). However, despite their excellent mechanical response to different loading conditions (Palomba, et al., 2021), the joint between sandwich panels and other metal components represents a critical aspect. One solution to this problem is to adhesively bond metal profiles to the composite structure in a prefabrication phase (Hentinen, et al., 1997). Kharghani and Guedes Soares (2018) tested a model of a composite-to-steel hybrid balcony overhang under shear and bending loads, outlining how the stiffness mismatch between the metal and composite part is one of the crucial parts in the structural design.

2.5 *Optimisation algorithms*

Various search and optimisation algorithms have been developed and can be classified into single-solution-based and population-based metaheuristic algorithms (Katoch, et al., 2021). The formers utilise a single candidate solution and improve this solution by using local search, which can be stuck in local optima. Population-based metaheuristics utilise multiple candidate solutions during the search process. A few examples: Genetic Algorithms (GA) (Holland, 1975), Vector-Evaluated Genetic Algorithms (VEGA) (Schaffer, 1985), and Particle Swarm Optimisation (PSO) (Kennedy & Eberhart, 1995).

A GA mimics evolutionary principles and chromosomal processing in natural genetics. GAs works iteratively by successively applying reproduction, crossover and mutation operators until a termination criterion is satisfied. These came into play with Holland (1975), during the first years mainly practised by Holland and his students (De Jong, 1975; Goldberg, 1983). GAs show great applicability to complex optimisation problems for their ability to represent the solutions in a set of Pareto-optimal points. Indeed, in a typical multi-objective optimisation problem, one solution may not exist that's best, and the suitability of one solution depends on several factors (Srinivas, et al., 1994).

Srinivas et al. (1994) developed a Non-Dominated Sorting Genetic Algorithm (NSGA) based on Goldberg's (1989) suggestion of a non-dominated sorting procedure. Deb et al. (2002) formulated a Fast Elitist Non-Dominated Sorting GA (NSGA-II) to overcome the main criticisms of NSGA.

2.6 *Structural optimisation*

The first formulation of a multi-objective optimisation problem was developed by Edgeworth (1881), and later extended to *n*-objectives by Pareto (1906).

The first optimisation application to ships only appeared with Harlander (1960), dealing with least-weight plate-stiffener arrangements for two different loading conditions. The implementation of computer optimisation problems was carried out later by Evans and Khoushy (1963) and Nowacki et al. (1970).

Nobuwaka and Zhou (1996) developed a discrete optimisation of ship structures applied to a cargo ship with a GA and investigated the influences of the penalty coefficient, population size, crossover probability and mutation probability on results and convergence of the. Jastrzebski and Sekulski (2005) applied a GA to the structural optimisation of a high-speed craft, considering a discrete set of scantlings for plates, bulb extrusions and T-bar extrusions. At this stage of development, optimisation problems only deal with one objective function at a time.

Rigo (2003) applied multi-objective optimisation to a cruise ship, intending to reduce the cost of production and the structure's weight.

Ultimate limit states were considered in the work of Hughes et al. (2014), who applied the VEGA to optimise the cargo hold of double-hull tankers. One year later, Ma et al. (2015) employed a PSO algorithm to optimise an isolated midship section of the same ship and extended the analysis to the ultimate strength of the midship section.

All previous concepts were implemented in Garbatov and Georgiev (2017) with a reliability-based optimisation of a stiffened plate subjected to combined stochastic compressive loads, accounting for the design's ultimate strength and reliability-based constraints. Three years later, Huang and Garbatov (2020) extended the concept to ship structures employing an NSGA-II, accounting for the local fatigue damage and ultimate global strength and mapping the Pareto frontier solutions with a FORM.

3 APPLICATION TO A MULTI-PURPOSE SHIP

The ship object of optimisation is a 9800 DWT multi-purpose ship, equipped for the carriage of containers, strengthened for heavy cargoes (Figure 1):

Table 1. Ship main dimensions

Property	Symbol	Value	Unit
Rule length	L	115.07	m
Breadth moulded	B	20.00	m
Depth moulded	D	10.40	m
Draught (scantling)	T	8.30	m
Block coefficient	C_B	0.719	

3.1 *Model*

Loads, hull girder strength and local hull scantling are determined according to DNV rules for the classification of ships (DNV, 2021). Additional steel sandwich panel construction requirements are found in DNV-CG-0154 (2021). The buckling check of steel structures is performed according to DNV (2009) Design. The buckling check of the honeycomb core sandwich panels is performed according to the Hexcel Composites (2000) manufacturer guide.

3.1.1 *Materials*

The hybrid structure is composed of standard shipbuilding steels with a yield strength from 235 to 390 N/mm^2 and AHS of aluminium alloy 5251-T3 (Table 2) replacing the vertical inner skin of the cargo hold:

Table 2. Assumed properties of structural materials

Property	Symbol	Value	Unit
Steel yield stress	$\sigma_{y,s}$	235 – 390	N/mm^2
Steel Young modulus	E_s	$2.05 \cdot 10^5$	N/mm^2
Poisson's ratio	v	0.33	-
Steel density	ρ_s	7800	kg/m^3
Aluminium yield stress	$\sigma_{y,\,al}$	235	N/mm^2
Aluminium Young modulus	E_s	$7.05 \cdot 10^4$	N/mm^2
Aluminium density	ρ_{al}	2700	kg/m^3

The contribution of AHS to strength calculations is considered with an equivalent single plate approach (Figure 2) (Paik, et al., 1999). This is performed by applying an equivalent rigidity method where in-plane tension, bending and shear are considered separately:

- In tension:

$$2t_f E_f = t_{eq,0} E_{eq} \tag{1}$$

- In bending:

$$\frac{1}{12}\left[\left(h_c + 2t_f\right)^3 - h_c^3\right] E_f = \frac{1}{12} t_{eq,0}^3 E_{eq} \tag{2}$$

- In shear:

$$2t_f G_f = t_{eq,0} G_{eq} \tag{3}$$

The equivalent single skin panel thickness $t_{eq,0}$ is obtained by solving the above equations, yielding:

$$t_{eq,\,0} = \sqrt{3h_c^2 + 6h_c t_f + 4t_f^2} \tag{4}$$

The equivalent single-skin panels are later transformed to obtain a midship section composed of homogeneous materials. By defining the ratio T = E_{al}/E_s between the Young modulus of aluminium and steel, the new equivalent thickness is found by Equation 5:

$$t_{eq} = \mathrm{T} \cdot t_{eq,0} \tag{5}$$

3.1.2 *Load cases*

The strength assessment is based on the combination of static plus dynamic load cases for full load conditions at a probability level of 10^{-8}.

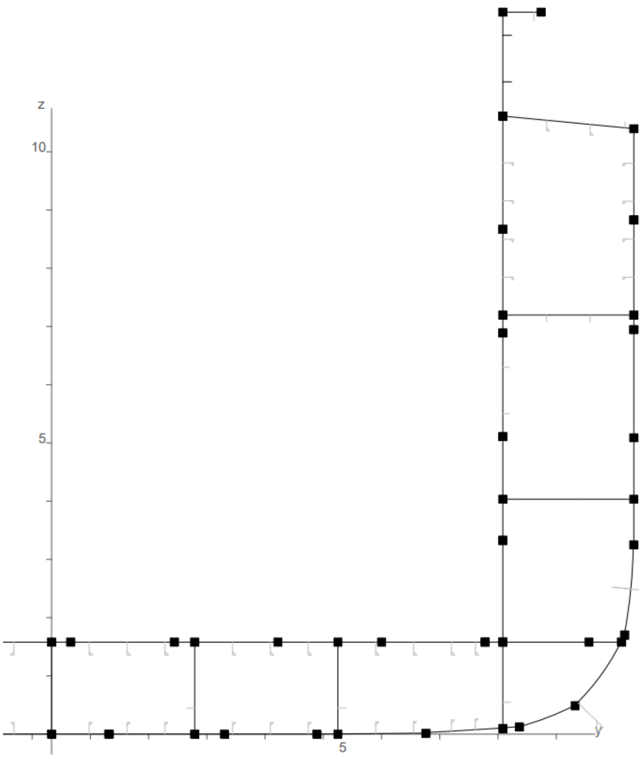

Figure 1. Half view of the midship section.

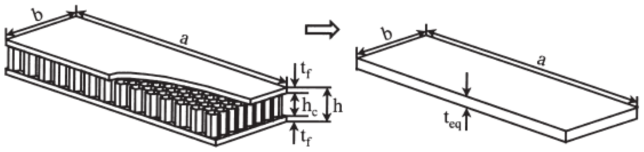

Figure 2. Equivalent single skin panel approach (Paik, et al., 1999)

The considered equivalent design waves to generate wave-induced dynamic load cases are HSM-2 and FSM-2, which maximise the vertical wave bending moment amidships for the head and following seas, respectively. The load combination factors (LCFs) are defined accordingly (DNV, 2021).

3.2 *Structural optimisation*

The multi-objective optimisation problem involves K≥1 criteria and can be formulated as (Parsons & Scott, 2004; Sharma, et al., 2012):

$$\begin{cases} \min\limits_{\boldsymbol{x}} \ \mathrm{F}_1(\boldsymbol{x}) = [f_1(\boldsymbol{x}), f_2(\boldsymbol{x}), f_3(\boldsymbol{x}), \dots, f_K(\boldsymbol{x})] \\ \max\limits_{\boldsymbol{x}} \ \mathrm{F}_2(\boldsymbol{x}) = [f_1(\boldsymbol{x}), f_2(\boldsymbol{x}), f_3(\boldsymbol{x}), \dots, f_K(\boldsymbol{x})] \end{cases} \quad (6)$$

Subject to the bounds on decision variables and equality and inequality constraints:

$$\begin{aligned} &\boldsymbol{x}^{\mathrm{L}} \le \mathbf{x} \le \mathbf{x}^{\mathrm{U}} \\ &h_i(\boldsymbol{x}) = 0, \quad \mathrm{i} = 1, \dots, \mathrm{I} \\ &g_i(\boldsymbol{x}) \ge 0, \quad \mathrm{j} = 1, \dots, \mathrm{J} \end{aligned} \quad (7)$$

There are now K multiple optimisation criteria $f_1(\mathbf{x})$ through $f_K(\mathbf{x})$, and each depends on the N unknown design parameters in the vector **x**. The overall cost function **F** is a vector. This problem has no solution due to conflicts among the K optimisation criteria. A design team typically seeks a single result that is a practical compromise or trade-off among the conflicting criteria.

Structural optimisation involves the interaction of multiple sub-processes interconnected together with the use of VBA. In the first stage, a ship's model is made as a function of the selected design variables. This model was later integrated into the EMOO developed by Sharma et al. (2012) and Wong et al. (2016). Finally, the solutions are exported to MARS 2000 for ultimate strength calculation, and the Pareto-optimal front is mapped with the FORM. This automation process is divided into the first part dealing with optimisation (Figure 3) and the second part dealing with the β-reliability index (Figure 4). Details about the flow chart involved in the MS Excel MOO program can be found in Sharma et al. (2017).

3.2.1 *Objective functions*

The identified objective functions are the ship's lightweight (LW), F_1 and the yield stress at the deck for sagging in seagoing conditions, F_2.

The regression formula can obtain the lightweight of the ship, as proposed by Garbatov et al. (2022):

$$\mathrm{LW} = 0.034 L^{1.7} B^{0.7} D^{0.4} C_B^{0.5} \left(0.2 + 0.8 \frac{W_{AHS,Steel}}{W_{Steel}}\right) \quad (8)$$

The longitudinal stress at the deck in sagging conditions, induced by still water and dynamic vertical hull girder bending, can be obtained by:

$$\sigma_d = \frac{M_{sw-s} + M_{wv}}{I_y}(z_d - z_n) \quad (9)$$

Where M_{sw-s} is the permissible vertical still water bending moment for, M_{wv} is the vertical wave bending moment, I_y is the net moment of inertia of the midship section about its horizontal neutral axis, z_d is the considered coordinate at the deck, and z_n is the coordinate of the horizontal neutral axis about the keel.

3.2.2 *Design Variables*

In this optimisation problem, fifty-eight discrete design variables (Table 3) have been identified and can be divided into seven categories:

i. Ship hull gross plates thicknesses;
ii. Sandwich panel gross thicknesses;
iii. Sandwich plate gross thicknesses;
iv. Steel bulb extrusions (Corus Special Profiles, 2002);
v. Span of the longitudinal members;
vi. Yield stress of steel;
vii. Cell density of AHS core (Table 4-Table 5).

The lower bound of steel and aluminium plate is determined by the minimum thickness requirements given by the rules, whereas the upper bound is set considering the type of the ship. Exception on the lower bound is made for variables x_{14} - x_{17}, where the minimum thickness is considered suitable for regular use of grabs of up to 10 tonnes of unladen weight, as indicated in the original midship section.

It is assumed that each stiffened plate panel is composed of homogeneous stiffeners, obtained by considering only the most loaded stiffener of each group to meet minimum scantling requirements and extend the scantling to the rest of the stiffeners.

Table 3. Design variables and their description.

Variable	Description	x^L mm	x^U mm	x_{step} mm
x_1	Bilge plate	11.5	18	0.5
x_2	Bottom plate no. 1	10	18	0.5
x_3	Bottom plate no. 2	10	18	0.5
x_4	Bottom plate no. 3	10	18	0.5
x_5	Bottom plate no. 4	10	18	0.5
x_6	Bilge plate no. 1	10	22	0.5
x_7	Bilge plate no. 2	10	22	0.5
x_8	Side shell plate no. 1	9.5	18	0.5
x_9	Side shell plate no. 2	9.5	18	0.5
x_{10}	Side shell plate no. 3	9.5	18	0.5
x_{11}	Side shell plate no. 4	9.5	18	0.5
x_{12}	Side shell plate no. 5	9.5	20	0.5
x_{13}	Deck plate no. 1	8	20	0.5
x_{14}	Inner bottom plate no. 1	15	18	0.5
x_{15}	Inner bottom plate no. 2	15	18	0.5
x_{16}	Inner bottom plate no. 3	15	18	0.5
x_{17}	Inner bottom plate no. 4	15	18	0.5
x_{18}	Central girder panel	8	18	0.5
x_{19}	Side girder panel no. 1	8	18	0.5
x_{20}	Side girder panel no. 2	8	18	0.5
x_{21}	Side girder panel no. 3	8	18	0.5
x_{22}	Lower stringer panel	7.5	18	0.5
x_{23}	Middle stringer panel	7.5	18	0.5
x_{24}	Upper stringer panel	7.5	18	0.5
x_{25}	Inner skin panel no. 1	20	60	0.5
x_{26}	Inner skin panel no. 2	20	60	0.5
x_{27}	Inner skin panel no. 3	20	60	0.5
x_{28}	Inner skin panel no. 4	20	60	0.5
x_{29}	Inner skin panel no. 5	20	60	0.5
x_{30}	Inner skin plate no. 1	5.5	10	0.5
x_{31}	Inner skin plate no. 2	5.5	10	0.5
x_{32}	Inner skin plate no. 3	5.5	10	0.5
x_{33}	Inner skin plate no. 4	5.5	10	0.5
x_{34}	Inner skin plate no. 5	5.5	10	0.5
x_{35}	Keel stiffener	1	59	1
x_{36}	Bottom stiffener no. 1	1	59	1
x_{37}	Bottom stiffener no. 2	1	59	1
x_{38}	Bottom stiffener no. 3	1	59	1
x_{39}	Bottom stiffener no. 4	1	59	1
x_{40}	Side shell stiffener no. 1	1	59	1
x_{41}	Side shell stiffener no. 2	1	59	1
x_{42}	Deck stiffener no. 1	1	59	1
x_{43}	Deck stiffener no. 2	1	59	1
x_{44}	Inner bottom stiffener no. 1	1	59	1
x_{45}	Inner bottom stiffener no. 2	1	59	1
x_{46}	Inner bottom stiffener no. 3	1	59	1
x_{47}	Inner bottom stiffener no. 4	1	59	1
x_{48}	Inner skin stiffener no. 1	1	59	1
x_{49}	Inner skin stiffener no. 2	1	59	1
x_{50}	Multiple stiffeners' spacing	3	5	1
x_{51}	Lower section material	1	4	1
x_{52}	Middle section material	1	4	1
x_{53}	Upper section material	1	4	1
x_{54}	Core cell density panel no. 1	1	7	1
x_{55}	Core cell density panel no. 2	1	7	1
x_{56}	Core cell density panel no. 3	1	7	1
x_{57}	Core cell density panel no. 4	1	7	1
x_{58}	Core cell density panel no. 1	1	7	1

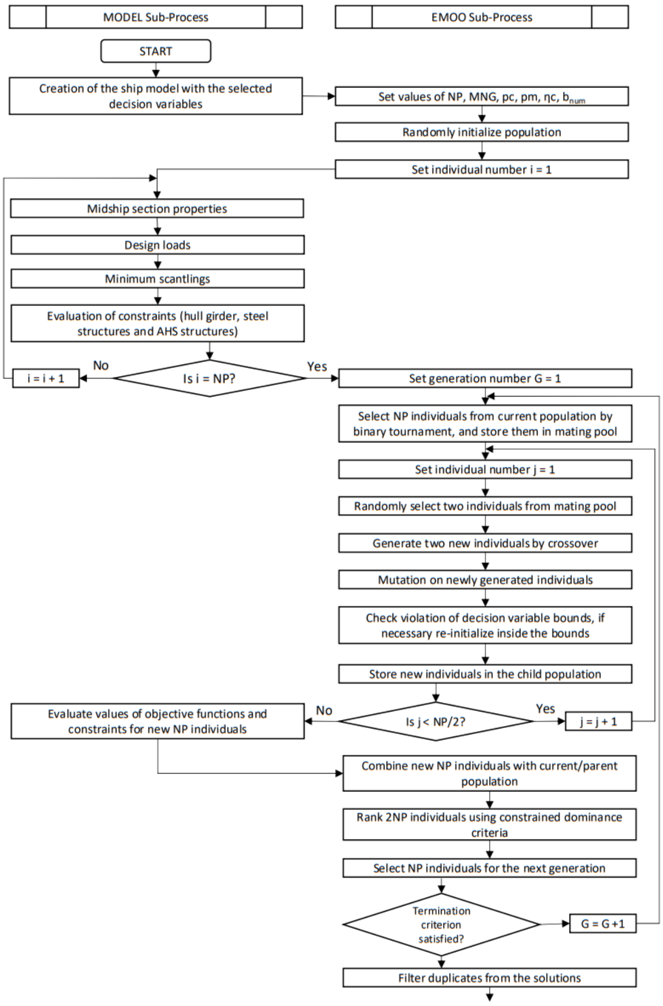

Figure 3. Optimisation Sub-process flowchart.

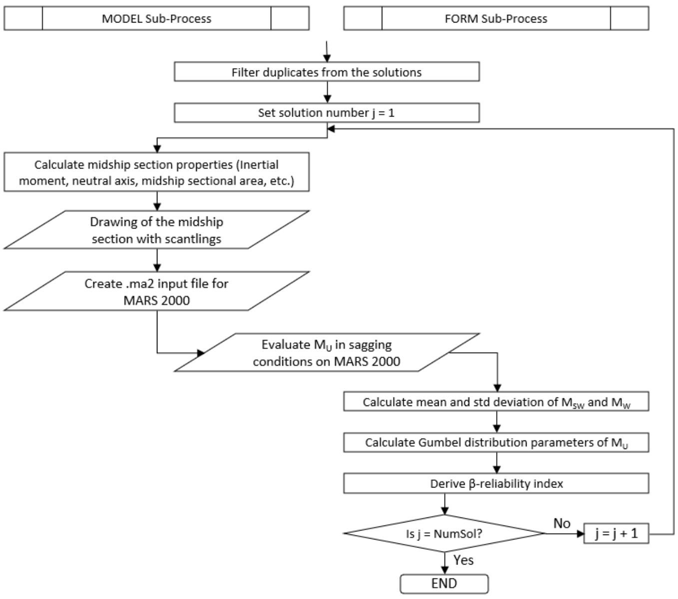

Figure 4. Reliability Sub-process flowchart.

Table 4. Mechanical properties of honeycomb core in compression (HexCel Composites, 2000).

Item	Density	Cell size	Strength	Modulus
	kg/m^3	in	N/mm^2	N/mm^2
1	37	0.25	1.4	310
2	50	0.19	2.3	517
3	54	0.25	2.6	620
4	72	0.13	4.2	1034
5	83	0.25	5.2	1310
6	127	0.25	10.0	2345
7	130	0.13	11.0	2414

Table 5. Mechanical properties of honeycomb core shear in longitudinal and transversal directions, respectively (HexCel Composites, 2000).

Item	Density	Strength (L)	Modulus (L)	Strength (W)	Modulus (W)
	kg/m^3	N/mm^2	N/mm^2	N/mm^2	N/mm^2
1	37	1.0	220.0	0.6	112.0
2	50	1.5	310.0	0.9	152.0
3	54	1.6	345.0	1.1	166.0
4	72	2.3	483.0	1.5	214.0
5	83	2.8	565.0	1.8	245.0
6	127	4.8	896.0	2.9	364.0
7	130	5.0	930.0	3.0	372.0

3.2.3 *Constraints*

The applicable constraints to the optimisation problem can be divided into three sets: hull girder, steel structures and AHS. Additionally, constraints on the coefficients introduced in AHS have been set to meet their domain of definition. The total number of identified constraints amounts to 167.

The constraints applicable to the hull girder are connected to the midship section and may be summarised as follows:

i. Inertial moment:

$$I_y - I_{Ry} \geq 0 \tag{10}$$

Where:

$$I_{Ry} = 3 f_r C_W L^3 \mathrm{B}(C_B + 0.7) \tag{11}$$

ii. Modulus at the bottom:

$$Z_B - I_{Ry}/z_n \geq 0 \tag{12}$$

iii. Modulus at deck:

$$Z_D - I_{Ry}/(D - z_n) \geq 0 \tag{13}$$

iv. Hull girder stress at the bottom:

$$\sigma_{al-b} - \frac{\max[(M_{sw-h} + M_{wv})\,;\ -(M_{sw-s} + M_{wv})]}{I_y} \cdot z_n \geq 0 \tag{14}$$

Where σ_{al} is the allowable stress:

$$\sigma_{al} = 205/k \tag{15}$$

v. Hull girder stress at deck:

$$\sigma_{al-d} - \frac{\max[(M_{sw-h} + M_{wv})\,;\ -(M_{sw-s} + M_{wv})]}{I_y} \cdot (D - z_n) \geq 0 \tag{16}$$

The set of constraints for steel structures relate to local scantling and buckling:

i. Minimum panel plate thickness:

$$t_i - t_{min} \geq 0 \tag{17}$$

ii. Minimum sectional area of bulb profile:

$$\mathrm{a} - 0.68 \sqrt[3]{Z_{min}^2} \geq 0 \tag{18}$$

iii. Minimum bilge thickness concerning adjacent plates:

$$\min(x_6, x_7) - \max(x_5, x_8) \geq 0 \tag{19}$$

iv. Minimum critical buckling stress σ_c:

$$\sigma_c - \frac{\sigma_{al}}{\eta} \geq 0 \tag{20}$$

Where σ_{al} is the compressive stress in plate panels, defined as:

$$\sigma_{al} = \frac{M_{SW} + M_{WV}}{I_y}(z_n - z_a) \tag{21}$$

Where z_a is the vertical distance from the baseline or deckline to the point below or above the neutral axis, z_n is the vertical distance from the baseline or decline to the neutral axis of the hull girder, whichever is relevant.

The constraints applicable to AHS relate to simply supported plate (Eq. 23-26) and end-load conditions (Eq. 27-32):

- Minimum sectional area of bulb profile:

$$a - 0.68\sqrt[3]{Z_{min}^2} \geq 0 \tag{22}$$

- Deflection:

$$\delta_{all} - \frac{2K_1 q b^4 \lambda}{E_f t_f h^2} \geq 0 \tag{23}$$

Where q is the uniformly distributed load, b is the panel width, E_f is the modulus of elasticity of the facing skin, t_f is the thickness of the facing skin, h is the distance between the facing skin centres and δ_{al} = 0.01l is the allowable deflection (DNV, 2021);

- Facing stress:

$$\sigma_f - \frac{K_2 q b^2}{ht} \geq 0 \tag{24}$$

Where $\sigma_f = \sigma_{y,al}$ is the tensile strength of aluminium 5251-T3 alloy;

- Core shear:

$$\tau_c - \frac{K_3 q b}{h} \geq 0 \tag{25}$$

Where K_1, K_2 and K_3 are coefficients based on the simply supported plate coefficient;

- Local compression:

$$\sigma_c - \frac{P}{A} \geq 0 \tag{26}$$

Where σ_c is the core compressive stress, P is the applied load, and A is the area of the applied load;

- Facing stress:

$$\sigma_f - \frac{P}{2t_f b} \geq 0 \tag{27}$$

- Panel buckling:

$$P_b - \frac{\pi^2 D}{l^2 + \frac{\pi^2 D}{G_c h b}} \geq 0 \tag{28}$$

Where G_c is the shear modulus in the direction of applied load, and D is the bending stiffness, given by:

$$D = \frac{E_f t_f h^2 b}{2} \tag{29}$$

- Shear crimping:

$$P_b - t_c G_c b \geq 0 \tag{30}$$

- Skin wrinkling:

$$\sigma_{CR} - 0.5\left(G_c E_c E_f\right)^{1/3} \geq 0 \tag{31}$$

Where $\sigma_{CR} = \sigma_{y,al}$ is the tensile strength of aluminium 5251-T3 alloy;

- Intracell buckling:

$$\sigma_{CR} - 2E_f \left(\frac{t_f}{s}\right)^2 \geq 0 \tag{32}$$

Where s is the cell size.

4 RESULTS AND DISCUSSION

4.1 *Pareto-optimal front*

The Pareto-optimal front obtained with the MS Excel MOO is scaled concerning the original steel structure values by assuming a Lightweight ratio $F_1/F_{1,0}$, with $F_{1,0}$ = 1909.9 tons, equal to the original ship's LW, and a yield stress ratio $F_2/F_{2,0}$, with $F_{2,0}$ = 310.6 N/mm^2, equal to the allowable stress using NV-40 steel (Figure 5).

The algorithm parameters are set equal to the original papers of the MS Excel MOO, except for the maximum number of generations, equal to 200. The optimisation runtime is approximately 22 min. The algorithm achieved a 16.1% lightweight reduction compared to the original ship.

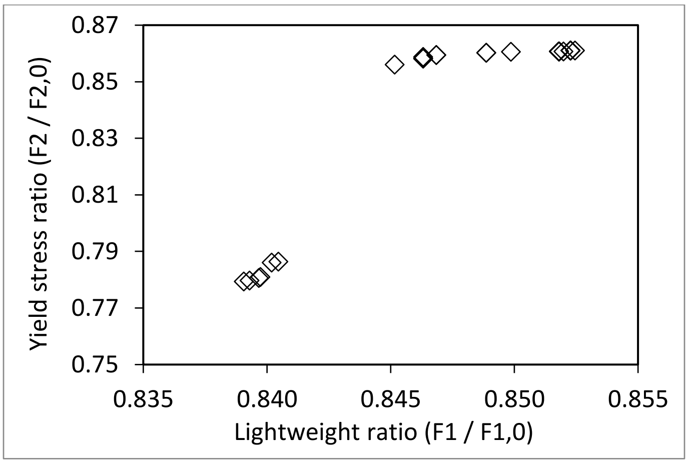

Figure 5. Pareto-optimal solutions.

4.2 *Ultimate Strength and Reliability*

The evaluation of the ultimate strength gives a better understanding of the post-buckling behaviour of the structure and, therefore, a more reliable design compared to the allowable stress design. The hull girder bending capacity at any hull transverse section must satisfy the following criterion:

$$M \leq \frac{M_U}{\gamma_R} \tag{33}$$

Where γ_R is a partial safety factor for the hull girder's ultimate bending capacity.

The ultimate bending capacity is assessed on MARS 2000 (2022), which makes use of the incremental-iterative method (IACS, 2021) to determine the bending moment M_i acting on the transverse section at each curvature χ_i. This is defined as the peak value of the M-χ curve (Figure 6) only considering vertical bending.

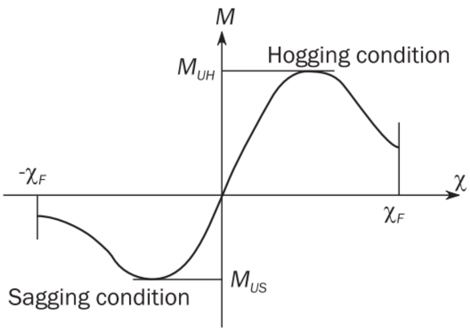

Figure 6. Bending moment capacity – curvature

The evaluation of the hull girder's reliability is based on its state of operation. This limit is called limit-state when the structure exceeds a specific limit and cannot operate safely. Ultimate limit-states are related to the structural collapse of part or all of the structure due to corrosion, fatigue, plastic mechanism, and progressive collapse.

The state of the structure can be described using resistance and load variables, $\mathbf{x} = (x_1,\ldots,x_n)$, and therefore, the limit-state function is a function $G(x_1,\ldots,x_n)$ of these variables, such that the limit-state equation separating the safe from the unsafe region is given by:

$$G(x_1, \ldots, x_n) = R - S = 0 \tag{34}$$

The failure condition, based on the resistance, R, and the load effect, S, is defined as:

$$R - S \leq 0 \tag{35}$$

Therefore, the probability of failure can be written as follows:

$$P_f = P[G(x_1, \ldots, x_n) \leq 0] \tag{36}$$

In general, there is not enough information on the distribution of the limit-state variables. Therefore, these are replaced with the statistical distribution.

The FORM method allows quantifying the structure's reliability with a β-reliability index, defined as the shortest distance from the origin to the transformed limit-state function into a standard normal space. This transformation can be achieved as follows:

$$\begin{aligned} U_1 &= \frac{R - E(R)}{\sigma_R}, \quad R = U_1\sigma_R + E(R) \\ U_2 &= \frac{S - E(S)}{\sigma_S}, \quad S = U_2\sigma_S + E(S) \end{aligned} \tag{37}$$

Where σ_i is the standard deviation, and $E(i)$ is the mean value. Finally, the β-reliability index is the solution to the constrained optimisation problem in the standard normal space:

$$\begin{aligned} &Minimise: && \beta(U) = \sqrt{U^T U} \\ &Subject\ to: && g(U) = 0 \end{aligned} \tag{38}$$

The limit-state function of the reliability assessment is based on the ship hull's ultimate strength, the vertical still water bending moment and the wave-induced bending moments, defined as:

$$G = \tilde{x}_U \cdot \widetilde{M}_U - \tilde{x}_{SW} \cdot \widetilde{M}_{SW} - \tilde{x}_W \tilde{x}_S \cdot \widetilde{M}_{WV} \tag{39}$$

Where M_U is the ultimate bending moment, M_{SW} is the still water bending moment, M_{WV} is the wave-induced bending moment, x_U is the model uncertainty on ultimate strength, x_{SW} is the uncertainty in the model of predicting the still water bending moment, x_W takes into account nonlinearities in sagging, and x_S is the error in the wave bending moment due to linear see keeping analysis. Parunov et al. (2015) introduced the variables representing the model uncertainty in their work on the structural reliability assessment of a container ship at the time of the accident (Table 6).

Table 6. Uncertainty factors in the limit-state function.

Parameter	Distribution	Mean	Standard deviation
x_U	Lognormal	1.10	0.11
x_{SW}	Normal	1.00	0.05
x_W	Normal	1.00	0.10
x_S	Normal	0.89	0.15

The ultimate bending moment is fitted to the Lognormal probability density function:

$$f_{M_U} = \frac{1}{M_U \sigma_{M_U\sqrt{2\pi}}} \cdot e^{-\frac{\ln\left(M_U - \mu_{M_U}\right)}{2\sigma^2_{M_U}}} \tag{40}$$

$$\sigma_{M_U} = \sqrt{\ln(COV^2 + 1)} \tag{41}$$

$$\mu_{M_U} \rightarrow F_{M_U}^{-1}(0.05, \mu_{M_U}, \sigma_{M_U}) = M_U^{5\%} \quad (42)$$

Where $M_U^{5\%}$ is the 5% confidence level ultimate bending moment calculated by MARS 2000, μ_{Mu} is the mean calculated iteratively for each M_U to return $M_U^{5\%}$, σ^2_{Mu} is the variance, and COV is the coefficient of variation assumed equal to 0.08.

The still water bending moment is fitted to the Normal distribution. Regression equations define the mean value and standard deviation of the still water bending moment as a function of the length of the ship and the dead-weight ratio, W = DWT/Full Load, as proposed by Guedes Soares and Moan (1988), Guedes Soares (1990):

$$\bar{M}_{SW,max} = 114.7 - 105.6W - 0.154L \quad (43)$$

$$\sigma(M_{SW,max}) = 17.4 - 7W + 0.035L \quad (44)$$

$$\bar{M}_{SW} = \frac{\bar{M}_{SW,max} \cdot M_{SW,CS}}{100} \quad (45)$$

$$\sigma(M_{SW}) = \frac{\sigma(M_{SW,max}) \cdot M_{SW,CS}}{100} \quad (46)$$

Where $\bar{M}_{SW}$ = 3.1 MNm is the mean still water bending moment, $\sigma(M_{SW,\,max})$ = 24.3 MNm is the still water bending moment standard deviation, W is assumed to equal to 0.9 for full load conditions, $M_{SW,\,CS}$ = -159.9 MNm is the still water bending moment.

The wave-induced bending moment for strength assessment, given by the Classification Societies Rules at a probability level of 10^{-8}, may be modelled as a Weibull distribution considering that the wave-induced bending moment can be represented as a stationary Gaussian process:

$$F_{M_{VW}} = 1 - \exp\left(\frac{M_{VW}}{q}\right)^h \quad (47)$$

Where q is the Weibull scale parameter, and h is the shape parameter, accordingly to DNV (2010):

$$q = \frac{M_{W,CS}}{\ln(10^8)^{1/h}} \quad (48)$$

$$h = 2.26 - 0.54\log_{10}(L) \quad (49)$$

The distribution of the extreme values of the wave-induced bending moment at a random point over a specified time period may be modelled as a Gumbel distribution (Guedes Soares, et al., 1996). The Gumbel distribution is derived from the Weibull factors as a function of the location parameter, α_m, and the scale parameter, β_m:

$$F_{M_W} = \exp\left\{-\exp\left(-\frac{M_{W,e} - \alpha_m}{\beta_m}\right)\right\} \quad (50)$$

$$\alpha_m = q(\ln(n))^h \quad (51)$$

$$\beta_m = \frac{q}{h}(\ln(n))^{(1-h)/h} \quad (52)$$

Where $M_{W,e}=(2\sigma^2_{Mw}\ln n)^{0.5}$ is a random variable representing the extreme values of the vertical wave-induced bending moment of the reference period, T_r. The number of cycles, n, is based on a reference time of one year for an average wave period T_W of 8 seconds:

$$n = \frac{p \cdot T_r \cdot 365 \cdot 24 \cdot 3600}{T_W} \quad (53)$$

Where p is the partial time in full load seagoing conditions, equal to 0.4.

The β-reliability indexes of the Pareto-optimal solutions (Table 7) are computed with VBA and compared with a target β-reliability index between 3.09 and 3.71 (DNV, 1992).

Table 7. β-reliability indexes of the Pareto-optimal solutions.

Sol. Num.	Light-weight ratio	Yield stress ratio	M_U MNm	α_m	β_m	β
1	0.839	0.779	810.1	926.8	74.1	4.43
2	0.839	0.780	808.7	925.1	74.0	4.42
5	0.840	0.781	803.1	918.8	73.5	4.39
7	0.840	0.781	802.7	918.3	73.5	4.38
10	0.840	0.786	785.1	898.2	71.9	4.27
11	0.840	0.786	785.1	898.2	71.9	4.27
12	0.845	0.856	724.8	829.2	66.3	3.87
17	0.846	0.858	695.9	796.1	63.7	3.67
18	0.846	0.859	694.0	794.0	63.5	3.66
19	0.847	0.859	700.5	801.4	64.1	3.70
21	0.849	0.860	690.3	789.8	63.2	3.63
22	0.850	0.861	687.8	786.9	62.9	3.61
24	0.852	0.861	681.3	779.4	62.4	3.57
28	0.852	0.861	681.1	779.2	62.3	3.57
29	0.852	0.861	687.6	786.6	62.9	3.61
31	0.852	0.861	687.6	786.7	62.9	3.61
33	0.852	0.861	687.3	786.2	62.9	3.61

The results show that the design optimisation tends to assume the properties of a single-objective optimisation, as the lighter design solutions are characterised by higher ultimate bending capacities and, therefore, higher β-indexes of reliability (Figure 7-Figure 8).

This can be justified by changing the midship sectional properties of the Pareto-optimal solutions. The selection of higher tensile strength steel at the bottom, and lower tensile strength at the deck, towards higher β-reliability indexes (Figure 9), impacts the structural members' scantling requirements. This selection contributes to a shift of the neutral axis towards the deck, positively impacting the buckling of structural members and, therefore, higher values of the ultimate bending capacity. The ultimate bending moment does not account for non-continuous structures, including hatch coaming and bilge keel. The contribution of these structures to the ultimate bending capacity needs to be evaluated by FEM analysis.

The obtained β-reliability indexes account for an average equivalent thickness of the sandwich panels of 22 mm. The model applied to sandwich panels tends to overestimate the ultimate bending capacity.

The midship section is made of two different materials, but artificially this is translated into a single homogeneous material, where no interaction between two panels of different materials is considered. AHS represent an excellent application for local pressure loads, as their core is parallel to the load. In the case of axial loads, the core does not contribute to the panel's strength. Therefore, the equivalent thickness approach does not represent the most suitable methodology for this problem. More analysis is needed for the honeycomb core subjected to axial pressure concerning buckling failure.

Furthermore, the redistribution of the axial loads between steel panel plates and AHS may not be smooth as considered. This aspect needs to be resolved in future studies.

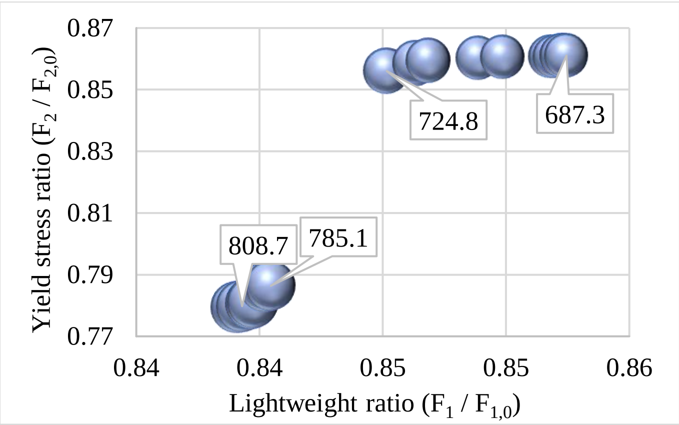

Figure 7. Ultimate bending capacity in MNm of the Pareto-optimal solutions in MNm.

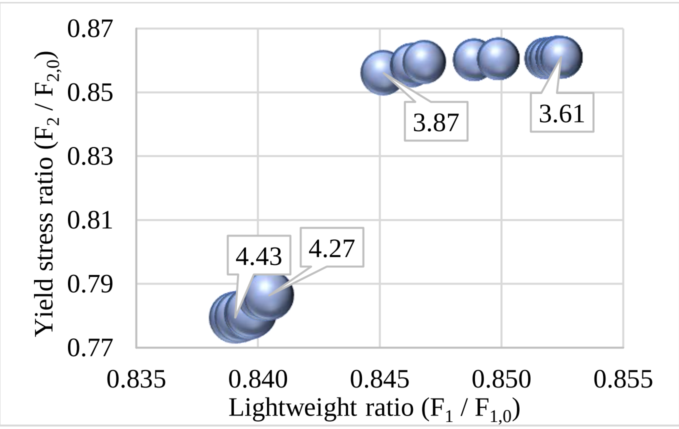

Figure 8. β-reliability indexes compared to target range 3.09 - 3.71

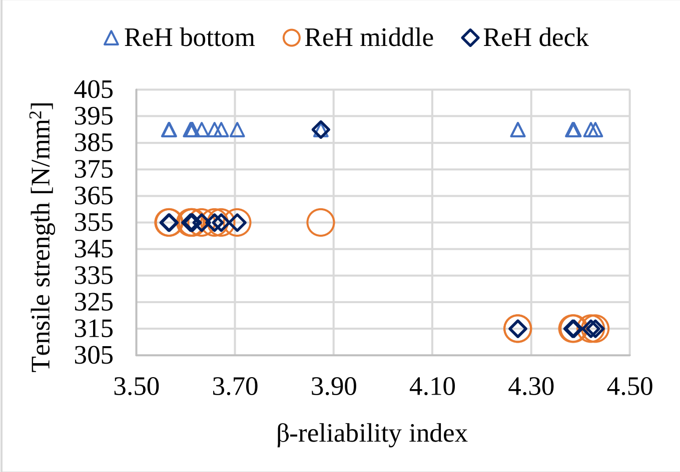

Figure 9. Steel tensile strength of the Pareto-optimal solutions

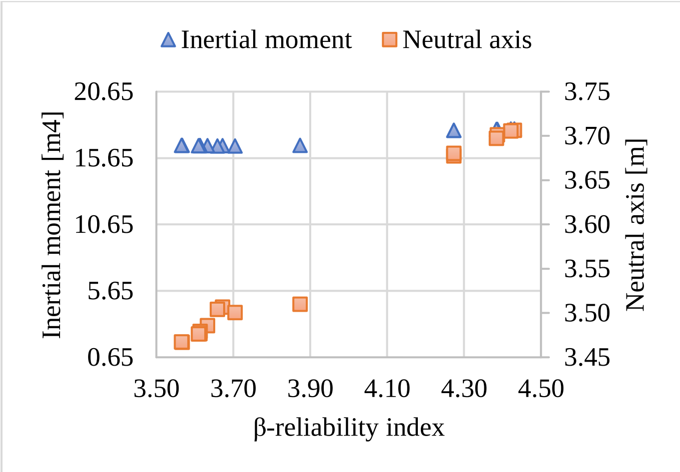

Figure 10. Inertial moment and position of the neutral axis of the Pareto-optimal solutions.

The capital cost assessment is based on the cost of steel and AHS. The cost of a sandwich panel of varying thicknesses of 3.2 m x 1.5 m is assumed as 520 EUR. The average weight of a sandwich panel is 200 kg, leading to a price of about 2600 EUR/ton. Together with the steel prices shown in Table 8, Equation 8 may be adapted as follows:

$$C_{Ship} = 0.034L^{1.7}B^{0.7}D^{0.4}C_B^{0.5}(0.2 \cdot \bar{C}_{steel} + 0.8(\%\mathrm{W_{AHS}} \cdot \mathrm{C_{AHS}} + (1 - \%W_{AHS}) \cdot \bar{C}_{steel})) \quad (54)$$

It is assumed that the cargo space represents 80% of the ship's length, where the AHS is employed. The cost of this portion considers the percentage of AHS weight in the midship section, $\%W_{AHS}$, to calculate the cost of the ship with the respective price of AHS. On average, this amounts to 7.2% of the midship section's weight (Table 9). The remaining part composed of steel considers an average cost among the steel prices in Table 8. The original ship cost equals 1,580,500 EUR.

Table 8. Detail of Steel and AHS prices (Made in China, 2022).

Item	Cost	Unit
235 N/mm^2 Steel	750	EUR/ton
315 N/mm^2 Steel	780	EUR/ton
355 N/mm^2 Steel	890	EUR/ton
390 N/mm^2 Steel	890	EUR/ton
AHS	2600	EUR/ton

Table 9. Economic assessment of the Pareto-optimal solutions.

Light-weight ratio	Yield stress ratio	β	LW Variation	W_{AHS}	C_{Ship}	Cost in-crease
			%	%	EUR	%
0.839	0.779	4.43	-16.1	6.8	1,765,700	11.7
0.839	0.780	4.42	-16.1	6.8	1,765,600	11.7
0.840	0.781	4.39	-16.0	6.8	1,765,500	11.7
0.840	0.781	4.38	-16.0	6.8	1,765,400	11.7
0.840	0.786	4.27	-16.0	6.9	1,768,000	11.9
0.840	0.786	4.27	-16.0	6.9	1,768,000	11.9
0.845	0.856	3.87	-15.5	7.4	1,781,800	12.7
0.846	0.858	3.67	-15.4	7.4	1,781,300	12.7
0.846	0.859	3.66	-15.4	7.4	1,781,300	12.7
0.847	0.859	3.70	-15.3	7.4	1,781,100	12.7
0.849	0.860	3.63	-15.1	7.5	1,782,300	12.8
0.850	0.861	3.61	-15.0	7.4	1,781,900	12.7
0.852	0.861	3.57	-14.8	7.3	1,778,700	12.5
0.852	0.861	3.57	-14.8	7.3	1,778,600	12.5
0.852	0.861	3.61	-14.8	7.4	1,781,300	12.7
0.852	0.861	3.61	-14.8	7.4	1,781,300	12.7
0.852	0.861	3.61	-14.8	7.4	1,781,200	12.7

5 CONCLUSION

A risk-based hybrid ship hull structural design optimisation was presented. The hybrid structure comprises honeycomb sandwich panels of aluminium 5251-T3 alloy replacing the vertical inner cargo shell. The optimisation is based on discrete variables employing a genetic algorithm, with ship lightweight and stress at the deck as objective functions. The optimisation aims to develop an automatic algorithm on VBA capable of joining the ship model, the EMOO software, the ultimate strength calculation with MARS 2000 and a β-reliability index code. The weight savings range between 14.8% - 16.1% concerning the original ship. High tensile steel of 390 N/mm^2 at the bottom and 315 N/mm2 steel at the midsection and deck contribute to lighter and more reliable solutions. The obtained β-reliability indexes range between 3.61 and 4.43; the values are deemed overestimated due to the equivalent thickness approach applied in the modelling of the AHS. A deeper understanding of the interaction between steel panel plates and AHS is required better to estimate the hull girder's ultimate bending capacity. The connection between these two structures creates problems due to the assumed redistribution of the axial loads to be smooth, which in reality, may be different. The honeycomb core is an excellent application for local pressure; however, more analysis is needed for the honeycomb core subjected to axial pressure concerning buckling failure. The material cost increase for the lightweight hybrid structure is about 12.4% considering an AHS cost of 2600 EUR/ton. The economic advantage of a hybrid structure requires additional investment analysis based on a ship's typical voyage and the expected duration of the investment.

Further studies in this direction could include ultimate bending capacity as the objective function by developing an incremental-iterative method code to be included as part of the VBA algorithm. Such code would require less than one hour to obtain a fully optimised structure. In the case of standard midship sections, the already developed algorithm is expected to obtain reliable solutions without overestimating the β-reliability indexes. Furthermore, the work presented could be implemented as software, including a user interface with drawing tools and a database of rules applicable to optimise different types of ships in a preliminary design stage.

6 REFERENCES

Allen, H. G., 1969. *Analysis and Design of Structural Sandwich Construction.* Oxford: Pergamon Press.

ANSYS, 2012. *Online Manuals. Release 12.* [Online].

Bitzer, T., 1994. Honeycomb Marine Applications. *Journal of Reinforced Plastics and Composites*, 13(4), p. 355–360.

Brand, P. R., Whitney, W. S. & Lewis, D. B., 1995. *Load and Resistance Factor Design Case Histories.* Houston, Texas, USA, OTC Offshore Technology Conference, pp. 637-643.

BS 4778, 1991. *Glossary of terms used in quality assurance (including reliability and maintainability terms).* London.

BV, 2022. *MARS 2000 (v. 2.9p).* [Online]
Available at: https://marine-offshore.bureauveritas.com/

Caldwell, J. B., 1965. Ultimate longitudinal strength. *Trans. RINA*, Volume 107, pp. 411-430.

Cornell, A. C., 1969. A probability-based structural code. *ACIJ*, 66(12), pp. 974-985.

Corus Special Profiles, 2002. [Online]
Available at: www.corus-specialprofiles.com
[Accessed 26 February 2022].

De Jong, K. A., 1975. *Analysis of the behaviour of a class of adaptive genetic systems (Doctoral Dissertation),* Ann Arbor: Department of Computer and Communication Sciences, University of Michigan.

Deb, K., Pratap, A., Agarwal, S. & Meyarivan, T., 2002. A fast and elitist multi-objective genetic algorithm: NSGA-II. *IEEE Transactions on Evolutionary Computation*, 6(2), pp. 182-197.

DNV, 1992. *Structural Reliability Analysis of Marine Structures. Classification Notes No. 30.6,* Norway: Det Norske Veritas.

DNV, 2009. *Hull structural design. Ships with length 100 metres above,* Norway: Det Norske Veritas.

DNV, 2010. *Fatigue Assessment of Ship Structures, Classification Notes No 30.7,* Norway: Det Norske Veritas.

DNV, 2021. *Rules for Classification of Ships,* Norway: Det Norske Veritas.

DNV-CG-0128, 2021. *Buckling,* Norway: Det Norske Veritas.

DNV-CG-0154, 2021. *Steel sandwich panel construction,* Norway: Det Norske Veritas.

Dorigo, M., Maniezzo, V. & Colorni, A., 1991. *Positive feedback as a search strategy. Tech. Rep. 91-016,* Milano: Dipartimento di Elettronica, Politecnico di Milano, Italy.

Edgeworth, F. Y., 1881. *Mathematical Psychics, an essay on the application of mathematics to the moral sciences, by F.Y. Edgeworth.* London: C.K. Paul.

Evans, J. H., 1959. Basic Design Concept. *Journal of the American Society for Naval Architects,* 71(4), pp. 671-678.

Evans, J. & Khoushy, D., 1963. Optimised Design of Midship Section Structure. *Trans. SNAME,* Issue 71, pp. 144-191.

Feng, G., Dongsheng, W., Garbatov, Y. & Guedes Soares, C., 2015. Reliability Analysis Based on a Direct Ship Hull Strength Assessment. *Journal of Marine Science and Application,* 14(04), pp. 389-398.

Feng, Y., Qiu, H., Gao, Y. & Zheng, H., 2020. Creative design for sandwich structures: a review. *International Journal of Advances Robotic Systems,* 17(3), pp. 1-24.

Garbatov, Y. & Georgiev, P., 2017. Optimal design of stiffened plate subjected to combined stochastic loads. In: *Progress in the Analysis and Design of Marine Structures.* London: Taylor & Francis Group, pp. 243-252.

Garbatov, Y., Scattareggia Marchese, S., Palomba, G. & Crupi, V., 2022. Alternative hybrid lightweight ship hull structural design. In: C. Guedes Soares & T. Santos, eds. *Trends in Maritime Technology and Engineering.* London: CRC Press, pp. 99-107.

Garbatov, Y., Sisci, F. & Ventura, M., 2018. Risk-based framework for ship and structural design accounting for maintenance planning. *Ocean Engineering,* Volume 166, pp. 12-25.

Glover, F. & Laguna, M., 1997. *Tabu search.* New York: Kluwer Academic Publishers.

Goldberg, D. E., 1983. *Computer-aided gas pipeline operation using genetic algorithms and rule learning (Doctoral Dissertation).* 3174B ed. Ann Arbor: University of Michigan.

Goldberg, D. E., 1989. *Genetic algorithms in search, optimisation and machine learning.* Reading, NY: Addison-Wesley.

Guedes Soares, C., 1990. Stochastic Modelling of Maximum Still-Water Load Effects in Ship Structures. *Journal of Ship Research,* Volume 34, pp. 199-205.

Guedes Soares, C. et al., 1996. Reliability-Based Ship Structural Design. *Trans. SNAME,* Volume 104, pp. 359-389.

Guedes Soares, C. & Moan, T., 1988. Statistical Analysis of Still-Water Load Effects in Ship Structures. *Trans. SNAME,* Volume 96, pp. 129-156.

Guedes Soares, C. & Teixeira, A. P., 2001. Risk assessment in maritime transportation. *Reliability Engineering & System Safety,* 74(3), pp. 299-309.

Harlander, L., 1960. Optimum Plate-Stiffener Arrangement for Various Types of Loading. *Journal of Ship Research,* 4(20), pp. 49-65.

Hasofer, A. M. & Lind, N. C., 1974. An exact and invariant first-order reliability format. *Journal of Engineering Mechanics Division,* Volume 100, pp. 111-121.

Hentinen, M., Hildebrand, M. & Visuri, M., 1997. *Adhesively bonded joints between FRP sandwich and metal: different concepts and their strength behaviour.* s.l.:VTT Tiedotteita - Valtion Teknillinen Tutkimuskeskus.

HexCel Composites, 2000. *HexWeb Honeycomb Sandwich Design Technology.* [Online]
[Accessed 2022].

Holland, J. H., 1975. *Adaptation in natural and artificial systems: An introductory analysis with applications to biology, control, and artificial intelligence.* Ann Arbor, Michigan, USA: University of Michigan Press.

Huang, Y. C. & Garbatov, Y., 2020. Multi-objective Reliability-Based Design of Ship Structures Subjected to Fatigue Damage and Compressive Collapse. *Journal of Offshore Mechanics and Arctic Engineering,* Volume 142(5), pp. 051701-1 - 051701-6.

Hughes, O. F. & Paik, J. K., 2010. *Ship Structural Design and Analysis.* New Jersey: The Society of Naval Architects and Marine Engineers.

Hughes, O., Ma, M. & Paik, J. K., 2014. *Applications of Vector Evaluated Genetic Algorithms (VEGA) in Ultimate Limit State Based Ship Structural Design.* San Francisco, California, USA, s.n., pp. 1-9.

Hughes, O., Mistree, F. & Zanic, V., 1980. A Practical Method for the Rational Design of Ship Structures. *Journal of Ship Research,* 24(2), pp. 101-113.

IACS, 2021. *Common Structural Rules for Bulk Carriers and Oil Tankers.*

IMO, 1966. *International Convention on Load Lines,* London.

IMO, 1993. *International Management Code for the Safe Operation of Ships and for Pollution Prevention (International Safety Management (ISM) Code). Resolution A.741(18),* London.

IMO, 1997. *Interim Guidelines for the Application of Formal Safety Assessment (FSA) to the IMO Rule-Making Process, MSC/Circ. 829 (MEPC/Circ. 335),* London.

IMO, 2002. *Guidelines for Formal Safety Assessment (FSA) for Use in the IMO Rule-Making Process. MSC/Circ.1023, MEPC/Circ.392,* London.

IMO, 2006. *FSA-Report of the Correspondence group MSC 81/18,* London.

IMO, 2008. *Formal safety assessment on crude oil tankers,* London.

IMO, 2009. *Hong Kong International Convention for the Safe and Environmentally Sound Recycling of Ships.*

IMO, 2011. *Resolution MEPC.203(62),* London.

IMO, 2013. *Revised guidelines for formal safety assessment (FSA) for use in the IMO rule-making process. MSC-MEPC.2/Circ.12.* London.

IMO, 2018. *Revised Guidelines for Formal Safety Assessment (FSA) for Use in the IMO Rule-Making Process. MSC-MEPC.2/Circ.12/Rev.2.* London.

ISO 8402, 1994. *International Standards Organization.* s.l.:s.n.

ISSC, 2003. *Committee III.1 – Ultimate Strength.* San Diego: International Ship and Offshore Structures Congress.

Jastrzebski, T. & Sekulski, Z., 2005. Application of genetic algorithm to structural optimisation of high-speed craft. In: *Maritime Transportation and Exploitation of Ocean and Coastal Resources.* London, UK: Taylor & Francis Group, pp. 859-866.

Katoch, S., Chauhan, S. & Kumar, V., 2021. A review on genetic algorithm: past, present, and future. *Multimedia Tools and Applications*, Volume 80, pp. 8091-8126.

Kelsey, S., Gellatly, R. A. & Clark, B. W., 1958. The Shear Modulus of Foil Honeycomb Cores. *Aircraft Engineering and Aerospace Technology,* 30(10), pp. 294-302.

Kennedy, J. & Eberhart, R., 1995. *Particle Swarm Optimisation.* Perth, Australia, pp. 1942-1948.

Kharghani, N. & Guedes Soares, C., 2018. Experimental and numerical study of hybrid steel-FRP balcony overhang of ships under shear and bending. *Marine Structures*, Volume 60, pp. 15-33.

Kharghani, N. & Guedes Soares, C., 2018. Experimental and numerical study of hybrid steel-FRP balcony overhang of ships under shear and bending. *Marine Structures,* Volume 60, pp. 15-33.

Kirpatrick, S., Gelatt, C. D. & Vecchi, M. P., 1983. Optimisation by simulated annealing. *Science*, 220(4598), pp. 671-680.

Klanac, A. & Jelovica, J., 2007. *A concept of omni-optimisation for ship structural design.* Glasgow, UK, Advancements in Marine Structures - Proceedings of MARSTRUCT 2007, The 1st International Conference on Marine Structures, pp. 473-482.

Kobayashi, H., Daimaruya, M. & Okuto, K., 1994. Elasto-Plastic Bending Deformation of Welded Honeycomb Sandwich Panel. *JSME International Journal*, 60(572), pp. 1011-1016.

Kujala, P. & Klanac, A., 2005. Steel Sandwich Panels in Marine Applications. *Brodogradnja: Teorija i praksa brodogradnje i pomorske tehnike,* 56(4), pp. 305-314.

Made in China, 2022. *www.made-in-china.com.* [Online] [Accessed July 2022].

MAESTRO Marine LLC Software, v11.2. [Online] Available at: https://www.maestromarine.com/

Mahfoud, M. & Emade, D., 2010. Aluminium Recycling - Challenges and Opportunities. *Advanced Materials Research*, Volume 83.86, pp. 571-578.

Ma, M., Hughes, O. & McNatt, T., 2015. *Ultimate Limit State-Based Ship Structural Design Using Multi-Objective Discrete Particle Swarm Optimisation.* St. John's, Newfoundland, Canada, pp. 1-10.

MARPOL, 1973. *International Convention for the Prevention of Pollution from Ships (MARPOL 73/78).* London.

MSA, 1993. *Formal safety assessment MSC66/14, Submitted by the United Kingdom to IMO Maritime Safety Committee.*

Nepomuceno de Oliveira, M. A., Szklo, A. & Castelo Branco, D. A., 2022. Implementing Maritime Transport Mitigation Measures according to their marginal abatement costs and mitigation potentials. *Energy Policy,* Volume 160, p. 112699.

Nobuwaka, H. & Zhou, G., 1996. Discrete Optimisation of Ship Structures with Genetic Algorithms. *Journal of The Society of Naval Architects of Japan,* Volume 179, pp. 293-301.

Nowacki, H., Brusis, F. & Swift, P., 1970. Tanker Preliminary design – An Optimisation Problem with Constraints. *Trans. SNAME,* Issue 78, pp. 357-390.

Okada, T. & Neki, I., 1992. Utilisation of genetic algorithm for optimising the design of ship hull structures. *Journal of The Society of Naval Architects of Japan 171,* pp. 71-83.

Okuto, K., Namba, K., Mizukoshi, H. & Hiyama, Y., 1991. The analysis and design of honeycomb welded structure. *J Light Met Welding,* 29(8), pp. 361-8.

Paik, J. K., 2003. ALPS/HULL User's Manual, A Computer Program for the Progressive Collapse Analysis of Ship Hulls. *Ship Structural Mechanics Laboratory.*

Paik, J. K. & Mansour, A. E., 1995. A simple formulation for predicting the ultimate strength of ships. *Marine Science and Technology,* Volume 1, pp. 52-62.

Paik, J. K., Thayamballi, A. K. & Gyu Sung, K., 1999. The strength characteristics of aluminium honeycomb sandwich panels. *Thin-Walled Structures,* Volume 35, pp. 205-231.

Palaversa, M., Prebeg, P. & Andric, J., 2020. Current State of Development of Ship Structural Design and Optimisation Methods. *Journal of Maritime & Transportation Science,* 3(3), pp. 171-187.

Palomba, G., Epasto, G., Sutherland, L. & Crupi, V., 2021. Aluminium honeycomb sandwich as a design alternative for lightweight marine structures. *Ships and Offshore Structures,* pp. 1-12.

Papanikolaou, A. & Konovessis, D., 1999. *Safety in Ship Design: Review of Fundamental Concepts and Methodologies.* Glasgow, UK, s.n., pp. 23-42.

Pareto, V., 1906. *Manuale di economia politica: con una introduzionea alla scienza sociale.* Milano: Società Editrice Libraria.

Parsons, M. G. & Scott, R. L., 2004. Formulation of Multi criterion Design Optimisation Problems for Solution with Scalar Numerical Optimisation Methods. *Journal of Ship Research,* 48(1), pp. 61-76.

Parunov, J., Andric, J. C. M. & Kitarovic, S., 2015. Structural reliability assessment of container ship at the time of accident. *Journal of Engineering for the Maritime Environment,* 229(2), pp. 111-123.

Parunov, J. & Guedes Soares, G., 2008. Effects of Common Structural Rules on hull-girder reliability of an Aframax oil tanker. *Reliability Engineering and System Safety*, Volume 93, pp. 1317-1327.

Plantema, F. J., 1966. *Sandwich Construction.* New York: Pergamon Press.

Qin, Z. & Batra, R. C., 2009. Local slamming impact of composite sandwich hulls. *International Journal of Solids and Structures,* Volume 46, pp. 2011-2035.

Rackwitz, R. & Fiessler, B., 1978. Structural Reliability under Combined Random Load Sequences Computers and Structures. *Computers and Structures,* 9(5), pp. 489-494.

Rausand, M., 1998. Introduction to Reliability Engineering. In: *Risk and Reliability in Marine Technology.* Rotterdam, NL: Balkema, pp. 371-381.

Rigo, P., 2001. A module-oriented tool for optimum design of stiffened structures – Part I. *Marine Structures,* Volume 14, pp. 611-629.

Rigo, P., 2003. An Integrated Software for Scantling Optimisation and Least Production Cost. *Ship Technology Research,* 50(3), pp. 125-140.

Schaffer, J. D., 1985. *Multi-objective optimisation with vector-evaluated genetic algorithms.* Hillsdale, New Jersey, Lawrence Erlbaun Associates, pp. 93-100.

Sharma, S., Rangaiah, G. P. & Cheah, K. S., 2012. Multi-objective optimisation using MS Excel with an Application to Design of a Falling-film Evaporator System. *Food and Bioproducts Processing,* 90(2), pp. 123-134.

Sharma, S., Rangaiah, G. P. & Cheah, K. S., 2012. Multi-objective optimisation using MS Excel with an Application to Design of a Falling-film Evaporator System. *Food and Bioproducts Processing,* 90(2), pp. 123-134.

Sharma, S., Rangaiah, G. P. & Marechal, F., 2017. Multi-objective optimisation Programs and Their Application to Amine Absorption Process Design for Natural Gas Sweetening. In: G. P. Rangaiah, ed. *Multi-objective optimisation: Techniques and Application in Chemical Engineering.* Singapore: World Scientific, pp. 533-560.

Smith, C., 1977. *Influence of Local Compressive Failure on Ultimate Longitudinal Strength of a Ship Hull.* Tokyo, JPN, pp. 73-79.

SOLAS, 1914-1974. *International Convention for the Safety of Life at Sea.* London.

Spouge, J., 1989. The Safety of Ro-Ro Passenger Ferries. *Trans. SNAME,* Volume 131.

Srinivas, N., Deb, K. & Deb, K., 1994. Multi-objective Optimisation Using Nondominated Sorting in Genetic Algorithms. *Evolutionary Computation,* 2(3), pp. 221-248.

Teixeira, A. P. & Guedes Soares, C., 2005. *Assessment of partial safety factors for the longitudinal strength of tankers.* Lisbon, Francis and Taylor, pp. 1601-1610.

Teixeira, A. P. & Guedes Soares, C., 2007a. Economical and social criteria for risk acceptance. In: *Public and Industrial Risks (in Portuguese).* Lisbon, Portugal: Edições Salamandra, Lda., pp. 45-63.

Teixeira, A. P. & Guedes Soares, C., 2007b. Economical considerations in establishing an optimal safety level for structures. In: *Public and Industrial Risks (in Portuguese).* Lisbon, Portugal: Edições Salamandra, Lda., pp. 623-642.

Tekgoz, M. & Garbatov, Y., 2020. Strength Assessment of Rectangular Plates Subjected to Extreme Cyclic Load Reversals. *Journal of Marine Science and Engineering,* 8(2), pp. 1-21.

Tekgoz, M. & Garbatov, Y., 2021. Collapse Strength of Intact Ship Structures. *Journal of Marine Science and Engineering,* 9(10), p. 1079.

Tekgoz, M., Garbatov, Y. & Guedes Soares, C., 2015. Ultimate strength assessment of a container ship accounting for the effect of neutral axis movement. In: *Maritime Technology and Engineering.* London, UK: Taylor & Francis Group, pp. 417-423.

Ueda, Y. & Rashed, M. H., 1984. The Idealised Structural Unit Method and its Application to Deep Girder Structures. *Computers and Structures,* 18(2), pp. 277-293.

United Nations, 1948. *Convention on the International Maritime Organisation.* Geneva.

Vinson, J. R., 1999. *The behaviour of sandwich structures of isotropic and composite materials.* Lancaster, Pennsylvania: Technomic.

Wang, J., 1994. *Formal safety analysis methods and their application to the design process.* UK: University of Newcastle Upon Tyne.

Wang, J., 2006. Maritime Risk Assessment and its Current Status. *Quality and Reliability Engineering International,* 22(1), pp. 3-19.

Wang, J. et al., 2004. Use of Advances in Technology for Maritime Risk Assessment. *Risk Analysis,* 24(4), pp. 1041-1063.

Wang, J., Yang, J. B., Sen, P. & Ruxton, T., 1996. Safety-based design and maintenance optimisation of large marine engineering systems. *Applied Ocean Research,* 18(1), pp. 13-27.

Wong, J. Y. Q., Sharma, S. & Rangaiah, G. P., 2016. Design of Shell-and-Tube Heat Exchangers for Multiple Objectives Using Elitist Non-dominated Sorting Genetic Algorithm with Termination Criteria. *Applied Thermal Engineering,* Volume 93, pp. 888-899.

Yeh, W. N. & Wu, Y. E., 1991. Enhancement of buckling characteristics for sandwich structure with fibre-reinforced composite skins and core made of aluminium honeycomb and polyurethane foam. *Theoretical and Applied Fracture Mechanics,* Volume 15, pp. 63-74.

Zenkert, D., 1993. *An Introduction to Sandwich Construction.* s.l.:Department of Lightweight Structures, Royal Institute of Technology.

Zenkert, D., Shipsha, A., Bull, P. & Hayman, B., 2005. Damage tolerance assessment of composite sandwich panels with localised damage. *Composites Science And Technology,* 65(15-16), pp. 2597-2611.